

# Transparent ZnAl<sub>2</sub>O<sub>4</sub> ceramics fabricated by spark plasma sintering

Byung-Nam KIM,<sup>†</sup> Keijiro HIRAGA,\* Ahrong JEONG,\*\* Chungfeng HU,  
Tohru S. SUZUKI, Jon-Do YUN\*\* and Yoshio SAKKA

National Institute for Materials Science, 1-2-1 Sengen, Tsukuba, Ibaraki 305-0047, Japan

\*Kitami Institute of Technology, 165 Koen-cho, Kitami, Hokkaido 090-8507, Japan

\*\*Kyungnam University, 449 Woryeong-dong, Changwon 631-701, Korea

**Highly transparent zinc aluminate ceramics were fabricated by the solid-state reaction using a spark plasma sintering machine. The sintered body exhibited a microstructure consisting of submicron-sized grains and extremely low porosities. Annealing of the sintered body in air improved the transmission close to the theoretical limit in a wavelength range of 1–5 μm. The band gap energy estimated from the absorption coefficient was 4.3 eV. The Young's modulus and the bulk modulus measured for the fully dense zinc aluminates were 282 and 211 GPa, respectively.**

©2014 The Ceramic Society of Japan. All rights reserved.

Key-words : Transmission, Zinc aluminate, Band gap energy, Elastic property, Spark plasma sintering, Annealing

[Received April 25, 2014; Accepted June 20, 2014]

## 1. Introduction

Zinc aluminate (ZnAl<sub>2</sub>O<sub>4</sub>, ZA) with a spinel structure has a combination of desirable properties such as high mechanical resistance, hydrophobic behavior, high thermal and chemical stability.<sup>1)</sup> Due to these properties, it is widely used as ceramic, electronic and catalytic materials. For the preparation of ZA powder, many methods have been proposed such as a solid-state reaction of ZnO and Al<sub>2</sub>O<sub>3</sub>,<sup>2)</sup> coprecipitation,<sup>3)</sup> hydrothermal<sup>4)</sup> and sol-gel method.<sup>5)</sup> Zinc aluminate is also one of the most important functional oxides with a wide band gap (3.8 eV), which is transparent to light of wavelengths above 320 nm.<sup>6)</sup> The ZA ceramics in a transparent form would be suitable for optical and optoelectronic applications. On the sintering of ZA, however, only a few studies have been reported, and most of the ZA ceramics have a relative density lower than 95%.<sup>2),7)-10)</sup> Fully dense transparent ZA was only recently fabricated by Goldstein et al.<sup>10)</sup> They applied hot isotropic pressing (HIP) to a nano-sized ZA powder. Owing to the optically isotropic property of ZA, a high density is the key for transparency. This study aimed to fabricate fully dense and highly transparent ZA with submicron-sized grains using the solid-state reaction by spark plasma sintering,<sup>11),12)</sup> and to examine optical and elastic properties of the sintered material.

## 2. Experiments

Commercial ZnO (205532, Aldrich, USA) and α-Al<sub>2</sub>O<sub>3</sub> powder (TM-DAR, Taimei Chemicals, Japan) were used with a molar ratio of 1:1. The ZnO powder with a purity of 99.9% and a particle size of <1 μm was mixed in ethanol with the Al<sub>2</sub>O<sub>3</sub> powder with a purity of 99.99% and a particle size of 0.15 μm. After drying and granulation using a 60-mesh sieve, the mixed powder was poured into a graphite die, and pressed by a graphite punch. The graphite die was heated to 800°C at a rate of

50°C/min, and then to the sintering temperature (1200°C) at a rate of 10°C/min using a spark plasma sintering machine (SPS-1050, Sumitomo, Japan). The temperature was measured by an optical pyrometer focused on the non-through hole on the graphite die. A uniaxial pressure of 80 MPa was applied from the beginning of the running. After holding for 20 min at the sintering temperature, we released the applied load and cooled down the graphite die at a rate of 10°C/min. At 1000°C, a power was turned off, and finally a sintered disk was obtained with a diameter of 10–30 mm and a thickness of 2–6 mm. During the running of SPS, the vacuum level was kept below 10<sup>-3</sup> torr.

For the measurement of optical properties, the sintered body was ground to a thickness of 1 mm and carefully mirror-polished on both sides using a diamond slurry. Subsequently, the polished samples were annealed at 1100°C for 3 h in air. The in-line transmission, total forward transmission and reflection were measured in the wavelength range of 240–1600 nm using a double-beam spectrophotometer (SolidSpec-3700DUV, Shimadzu, Japan) equipped with an integrating sphere. The distance between the sample and the detector is about 55 cm. The measurement of the in-line transmission was conducted by inserting a mask with a 2-mm diameter aperture in front of the detector in order to allow the detection of only the specularly transmitted portion of the incident light beam with a 4-mm diameter. Since the aperture diameter (2 mm) of the mask is smaller than the beam diameter (4 mm), only the light with a scattering angle less than 0.3° is detected. The transmission in the infrared wavelength region was also measured by using a fourier transform infrared spectroscopy (FT-IR) (Nicolet6700, Thermo Scientific, USA).

For the measurement of elastic properties, the sintered body was ground to a thickness of 5 mm and mirror-polished on both sides using a diamond slurry. With the 5-mm thick sample, a density was measured by the Archimedes' method, and the velocities of longitudinal and transverse waves were measured by the pulse-echo method. From the measured density and velocities, Young's modulus and the bulk modulus were calculated. The phases of the powder mixture and the sintered body

<sup>†</sup> Corresponding author: B.-N. Kim; E-mail: kim.byung-nam@nims.go.jp

were investigated by X-ray diffraction (XRD) (PINT-2500VHF, Rigaku, Japan).

For a specimen polished and thermally etched at 1100°C, microstructural observation was conducted using a scanning electron microscope (SEM) (JSM-6500, JEOL, Japan). The grain size was measured by obtaining the average cross section area per grain and by assuming spherical grains. The measured grain size is an apparent one, so that it was multiplied by 1.225 to determine the true grain size.<sup>13)</sup> Finally, the chemical composition was determined using an energy dispersive X-ray spectroscope (EDX).

### 3. Results and discussion

The synthesis of the ZA phase by the solid-state reaction was confirmed by XRD. After sintering, only the diffraction peaks of ZA were detected, and no other discernible peaks appeared, as shown in Fig. 1. During sintering, the powder mixture of ZnO and Al<sub>2</sub>O<sub>3</sub> reacted completely to form the single-phase ZA. The chemical composition of the sintered body determined by EDX is Zn<sub>x</sub>Al<sub>2</sub>O<sub>4</sub> ( $x = 1 \pm 0.05$ ). This molar ratio of ZnO and Al<sub>2</sub>O<sub>3</sub>, which is almost identical to that of the powder mixture, indicates that the volatility of ZnO is negligible during sintering. The XRD pattern for the powder mixture heated at 800°C was nearly identical to that of the sintered body. This result means that most reaction had been completed before primary densification and for this reason the volatility hardly occurred during sintering.

The microstructure of the sintered body is fine and dense, as shown in Fig. 2. The average grain size is 0.81 μm and the density is 4.59 g/cm<sup>3</sup>. The porosity measured from the SEM photographs taken at low magnification is 0.04%. Due to the low porosity, the sintered body appeared transparent, as shown in Fig. 3. The ZA ceramics sintered by SPS in vacuum appeared slightly darkish, but the annealing in air changed the sample whitish and improved the transparency, as in ZrO<sub>2</sub><sup>14)</sup> and Y<sub>2</sub>O<sub>3</sub>.<sup>15)</sup>

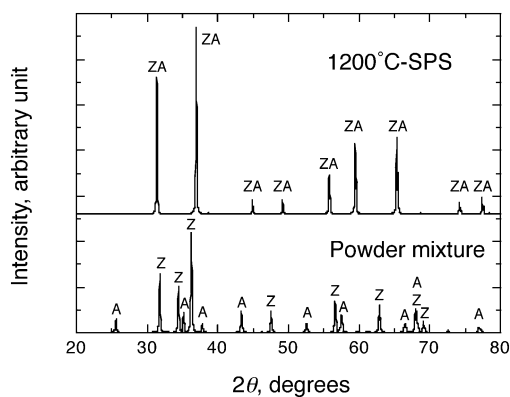


Fig. 1. XRD pattern for powder mixture and sintered body. Z, A and ZA represents ZnO, Al<sub>2</sub>O<sub>3</sub> and ZnAl<sub>2</sub>O<sub>4</sub>, respectively.

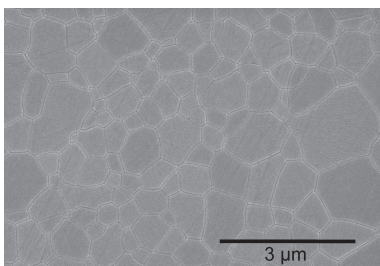


Fig. 2. Microstructure of sintered zinc aluminate.

The present ZA ceramics exhibited no cracks after both sintering and polishing even for samples of 30 mm diameter, whereas 80% of the ZA ceramics obtained by Goldstein *et al.*<sup>10)</sup> using HIP exhibited cracks after polishing. Hence, residual stresses seem to be lower for the present ZA than for the HIPed ZA.

The in-line transmission of the transparent ZA is shown in Fig. 4. The measured transmission has been converted for a 1 mm thick sample, using the refractive index reported by Medenbach and Shannon.<sup>16)</sup> The present in-line transmission is higher than that of the HIPed ZA, particularly in the visible wavelengths. For the HIPed ZA fabricated by Goldstein *et al.*, although the transmission reported in the literature<sup>10)</sup> is slightly higher than the present value, our measurement by the same method for the supplied sample yielded lower transmission, as shown in Fig. 4. Since the value of the in-line transmission increases with the allowance of scattering angle, the present method that allows scattering only less than 0.3° may yield the real in-line transmission. The higher transmission of the present ZA may arise from the higher density.

The in-line transmission was improved remarkably by annealing in air, as shown in Fig. 4. The improvement can mainly be attributed to the reduction of oxygen defects. For ZrO<sub>2</sub><sup>14)</sup> and Y<sub>2</sub>O<sub>3</sub><sup>15)</sup> fabricated by SPS, it was reported that annealing in air increases the scattering coefficient by forming pores and decreases the absorption coefficient by reducing oxygen defects. When the effect of decreased absorption surpasses the effect of the increased scattering, the annealing improves the transmission.<sup>14),15)</sup> A similar effect of annealing was also observed for the present ZA. The annealing effects on the absorption and scattering coefficients are shown in Fig. 5. The decrease in the absorption coefficient is remarkable in a wide wavelength range, particularly in the ultraviolet (UV) region (<400 nm), while the increase in the scattering coefficient is slight in the wavelength region of <500 nm. For this reason, the extinction (scattering +

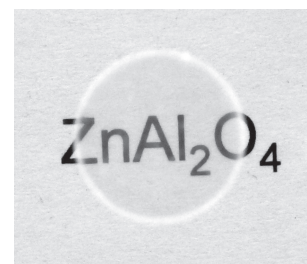


Fig. 3. Transparent ZA ceramics annealed at 1100°C for 3 h in air after sintering. The sample with diameter 10 mm and thickness 1.3 mm is 24 mm above the text.

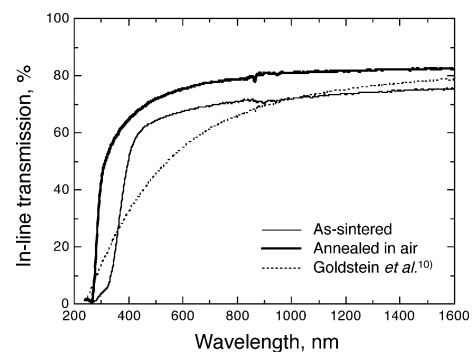


Fig. 4. In-line transmission after sintering and annealing. The measured transmission was converted for a thickness of 1 mm.

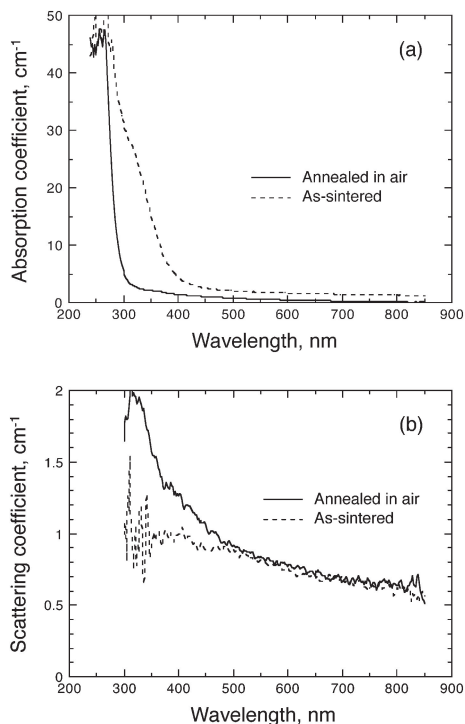


Fig. 5. (a) Absorption and (b) scattering coefficient before and after annealing.

absorption) decreased remarkably, and the in-line transmission was improved by the annealing.

From the absorption coefficient, the band gap energy can be estimated. A linear extrapolation to the wavelength axis in Fig. 5(a) yields a band gap of  $\sim 4.3$  eV (290 nm). The band gap for the annealed ZA ceramics is higher than the experimental value (3.8 eV) obtained for ZA powder,<sup>6</sup> but close to the value (4.0–4.5 eV) obtained for calcined ZA.<sup>1</sup> The present band gap is also close to the theoretical value (4.11 eV) calculated using the density functional theory.<sup>17</sup> The difference between the present and the theoretical band gap may be attributed to the slight difference in the chemical composition and to residual small pores. Light scattering by residual pores affects both the reflection and the total forward transmission, which are used for calculating the absorption coefficient, particularly in the UV region. On the other hand, the theoretical band gap obtained recently by Dixit et al.<sup>18</sup> using first-principle techniques is  $>6$  eV, the value of which is considerably higher than the experimental ones. The high band gap energy may explain the light transmission in the UV region for the transparent ZA obtained by Goldstein et al.,<sup>10</sup> as shown in Fig. 4. In the wavelength region of  $<270$  nm, whereas the present ZA is almost opaque, the ZA of Goldstein et al.<sup>10</sup> shows some transmissions. The light transmission in the UV region indicates low absorption coefficients and high band gap energies, although the related data were not shown in their work. Further studies are required for the optical properties in the UV region.

**Figure 6** shows the total forward transmission in a wide range of wavelength. By the annealing in air, the transmission was improved remarkably. In visible wavelengths, the transmission after annealing is close to a theoretical limit in the range of 1–5  $\mu\text{m}$ . For the wavelengths of  $>5$   $\mu\text{m}$ , the transmission is slightly higher than that of MgAl<sub>2</sub>O<sub>4</sub> spinel.<sup>19</sup> The absorption peak at 4.27  $\mu\text{m}$  is attributed to CO<sub>2</sub>.<sup>20</sup> We consider that the carbon diffused into the ZA from both carbon paper and mold during

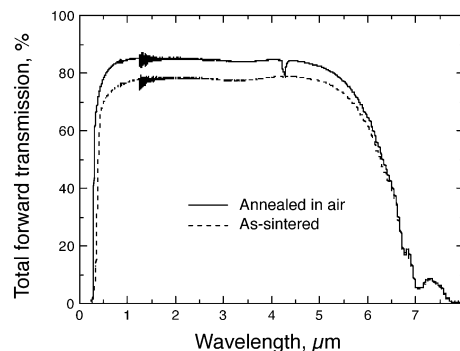


Fig. 6. Total forward transmission after sintering and annealing.

SPS reacted with oxygen during annealing in air, to form CO<sub>2</sub> gases. The gas formation within the ZA ceramics would accelerate the growth of pores, called swelling, which reduces the in-line transmission by increasing the scattering coefficient.

The Young's modulus and the bulk modulus measured for the transparent ZA are 282 and 211 GPa, respectively. The present bulk modulus is well consistent with the value (209 GPa) measured by the ultrasonic method for (Zn<sub>0.74</sub>Fe<sub>0.18</sub>Mg<sub>0.08</sub>)Al<sub>1.99</sub>O<sub>4</sub> single crystal<sup>21</sup> which has a spinel structure (gahnite), and is close to the value (202 GPa) measured by X-ray diffraction for ZnAl<sub>2</sub>O<sub>4</sub> powder.<sup>22</sup> The present Young's modulus also represents a good consistence with the value (268 GPa) obtained for (Zn<sub>0.74</sub>Fe<sub>0.18</sub>Mg<sub>0.08</sub>)Al<sub>1.99</sub>O<sub>4</sub> single crystal.<sup>21</sup> Since the present ZA has extremely low porosities, the elastic properties would be similar to those of the single crystal. On the other hand, van der Laag et al.<sup>9</sup> estimated the Young's modulus of 242 GPa for fully dense ZA, by an extrapolation from the values measured for sintered ZAs with low densities. As a result, their estimation yielded the Young's modulus much lower than the values for the present ZA and a gahnite single crystal. The present elastic properties for the fully dense ZA can be used in predicting various mechanical responses.

#### 4. Conclusions

Highly transparent zinc aluminate ceramics were fabricated by using spark plasma sintering. The transmission of the ZA was remarkably improved by annealing in air after sintering, and the improvement is attributed mainly to the reduction of the absorption coefficient. The optical band gap estimated from the absorption coefficient is  $\sim 4.3$  eV, which value is close to the prediction (4.11 eV) from the density functional theory. For the fully dense ZA, the Young's modulus and the bulk modulus were obtained to be 282 and 211 GPa, respectively.

**Acknowledgements** The authors thank to Dr. A. Goldstein for the supply of the HIPed zinc aluminate sample.

#### References

- 1) S. Mathur, M. Veith, M. Haas, H. Shen, N. Lecerf, V. Huch, S. Hufner, R. Haberkorn and H. P. Beck, *J. Am. Ceram. Soc.*, **84**, 1921–1928 (2001).
- 2) C. Leblud, M. R. Anseau, E. Di Rupo, F. Cambier and P. Fierens, *J. Mater. Sci. Lett.*, **16**, 539–544 (1981).
- 3) V. Ciupina, I. Carazeanu and G. Prodan, *J. Optoelectron. Adv. Mater.*, **6**, 1317–1322 (2004).
- 4) M. Zawadzki and J. Wryzyszczyk, *Mater. Res. Bull.*, **35**, 109–114 (2000).
- 5) L. K. Kurihara and S. L. Suib, *Chem. Mater.*, **5**, 609–613 (1993).

- 6) S. K. Sampath and J. F. Cordaro, *J. Am. Ceram. Soc.*, **81**, 649–654 (1998).
- 7) W.-S. Hong, L. C. De Jonghe, X. Yang and M. N. Rahaman, *J. Am. Ceram. Soc.*, **78**, 3217–3224 (1995).
- 8) D. Zhang, Z. Fu and J. Guo, *J. Mater. Sci. Technol.*, **19**, 526–528 (2003).
- 9) N. J. van der Laag, M. D. Snel, P. C. M. M. Magusin and G. de With, *J. Eur. Ceram. Soc.*, **24**, 2417–2424 (2004).
- 10) A. Goldstein, Y. Yeshurun, M. Vulfson and H. Kravits, *J. Am. Ceram. Soc.*, **95**, 879–882 (2012).
- 11) S. Grasso, Y. Sakka and G. Maizza, *Sci. Technol. Adv. Mater.*, **10**, 053001 (2009).
- 12) Z. A. Munir, D. V. Quach and M. Ohyanagi, *J. Am. Ceram. Soc.*, **94**, 1–19 (2011).
- 13) R. Apetz and M. P. B. van Bruggen, *J. Am. Ceram. Soc.*, **86**, 480–486 (2003).
- 14) H. B. Zhang, B.-N. Kim, K. Morita, H. Yoshida, J.-H. Lim and K. Hiraga, *J. Alloy Compd.*, **508**, 196–199 (2010).
- 15) H. B. Zhang, B.-N. Kim, K. Morita, H. Yoshida, K. Hiraga and Y. Sakka, *J. Am. Ceram. Soc.*, **94**, 3206–3210 (2011).
- 16) O. Medenbach and R. D. Shannon, *J. Opt. Soc. Am. B*, **14**, 3299–3318 (1997).
- 17) S. K. Sampath, D. G. Kanhere and R. Pandey, *J. Phys.: Condens. Matter*, **11**, 3635–3644 (1999).
- 18) H. Dixit, N. Tandon, S. Cottenier, R. Saniz, D. Lamoen, B. Partoens, V. Van Speybroeck and M. Waroquier, *New J. Phys.*, **13**, 063002 (2011).
- 19) G. C. Wei, *J. Phys. D Appl. Phys.*, **38**, 3057–3065 (2005).
- 20) M. P. Bernstein, D. P. Cruikshank and S. A. Sandford, *Icarus*, **179**, 527–534 (2005).
- 21) H. J. Reichmann and S. D. Jacobsen, *Am. Mineral.*, **91**, 1049–1054 (2006).
- 22) D. Levy, A. Pavese, A. Sani and V. Pischedda, *Phys. Chem. Miner.*, **28**, 612–618 (2001).